Spacecraft control with constrained fast reorientation and accurate pointing

G. Mengali and A. A. Quarta
Università di Pisa,
Dipartimento di Ingegneria Aerospaziale
Pisa, Italy

ABSTRACT

In this paper we study large angle rotational manoeuvres of spacecraft. The problem of attitude control is formulated and solved through potential functions, thus simplifying frequent reorientation manoeuvres. A combination of gas jet and FEEP thrusters is employed in order to obtain short settling times while meeting stringent pointing requirements. In this way, spacecraft reorientation is achieved in two integrated steps by means of a discrete/continuous control law. Autonomous avoidance of undesired space orientations is obtained and constraints due to the solar array pointing requirements are satisfied. A case study is discussed where the methodology is applied to a large space telescope.

NOMENCLATURE

$\boldsymbol{E}$	Euler's matrix
$\mathbf{i}, \mathbf{j}, \mathbf{k}$	body axes unit vectors
$\boldsymbol{I}$	inertia matrix
I_x, I_y, I_z	principal moments of inertia
k	design parameter
M_x, M_y, M_z	control torques
$\overline{M}_x, \overline{M}_y, \overline{M}_z$	gas jet torques
$\mathbf{n}$	pointing unit vector
0	spacecraft centre of mass
t	time
$\boldsymbol{T}$	coordinate transformation matrix
$T_B(x,y,z)$	body axes reference frame
$T_I(X,Y,Z)$	inertial frame
V	potential function
$\nabla(.)$	gradient operator: $\left[\frac{\partial(.)}{\partial\theta_1}\ \frac{\partial(.)}{\partial\theta_2}\ \frac{\partial(.)}{\partial\theta_3}\right]$
$\mathbf{x}$	state vector
Ω	angular velocity matrix
δ	slew angle
$\theta_1, \theta_2, \theta_3$	att. rates
ε	switching angle
η	design parameter
γ	solar array pointing angle
$\omega_x, \omega_y, \omega_z$	body rates
$\dot{\theta}_1, \dot{\theta}_2, \dot{\theta}_3$	att. angles
ϖ	shaping function
ω	angular velocity of spacecraft

Superscripts

$\cdot$	time derivative
$\wedge$	obstacle shaping parameter
d	desired
T	transposed

Subscripts

δ	slew angle dependent
♃	Jupiter
☾	Moon
ω	angular velocity dependent
☉	Sun
★	target
⊕	Earth
f	final condition
P	payload
p	design parameter
SA	solar array

Paper No. 2795. Manuscript received 5 September 2002, revised version received 7 March 2003, accepted 28 October 2003.

https://doi.org/10.1017/S0001924000005030 Published online by Cambridge University Press

1.0 INTRODUCTION

Large angle reorientation/slew manoeuvres are of primary importance in present and future spacecraft missions. In many circumstances it is mandatory that the sensitive payload does not intercept bright objects such as the sun, earth and moon, in order to avoid possible spacecraft damages. The subject of attitude manoeuvres avoiding forbidden directions has been considered in the past. Sorenson[1], for instance, used differential geometry to formulate pointing constraints and determine feasible attitude paths. Other approaches have been proposed by Frakes *at al*[2] and Singh *et al*[3]. More recently, Hablani[4] developed a general multi-axis avoidance path that guarantees that the seeker optics remain away from the radiant objects by a specified angle.

Following a different reasoning, potential function based methods have been proposed to simplify frequent reorientation manoeuvres of spacecraft with autonomous re-targeting capabilities[5]. An interesting feature of these methods is that the control torques are easily evaluated in closed form, thus facilitating the on-board implementation with reduced software requirements and clear advantages over other available approaches. The problem of attitude control using potential functions has been originally solved by means of continuous torque control. In a recent paper[6], the use of discrete on-off torques with gas jets has been considered. In both cases an important limitation exists in that the approach is only suitable for slewing the payload between targets and not for fine pointing.

In this paper the whole methodology is completely revisited and a new discrete/continuous control law is suggested which allows target re-positioning with accurate pointing capabilities. The reorientation problem is addressed in two integrated steps:

1. rapid slew manoeuvres are obtained through reaction jets with a typical tolerance of $0{\cdot}1^{o}$[7] and
2. the terminal fine pointing phase is left to FEEP thrusters that guarantee accurate thrust modulation in the 1μN–1m*N* range[8,9].

Autonomous avoidance of undesired space orientations is easily implemented and constraints imposed by the solar array pointing requirements are taken into account. The practical feasibility of the method is demonstrated by simulation.

2.0 EQUATIONS OF MOTION

Consider a body axes reference frame $T_B(x, y, z)$, where *x, y* and *z* are the principal axes of inertia of the spacecraft and let ***i, j, k*** the corresponding unit vectors. The rotational motion of the spacecraft about its center of mass 0 is described by the Euler's equations of motion

$$\begin{cases} M_x = I_x \dot{\omega}_x + (I_z - I_y)\,\omega_y\,\omega_z \\ M_y = I_y \dot{\omega}_y + (I_x - I_z)\,\omega_x\,\omega_z \\ M_z = I_z \dot{\omega}_z + (I_y - I_x)\,\omega_x\,\omega_y \end{cases} \quad \ldots (1)$$

where $M \equiv [M_x, M_y, M_Z]^T$ is the total external moment about 0, $\omega \equiv [\omega_x, \omega_y, \omega_z]^T$ is the angular velocity of the spacecraft relative to an inertial frame $T_I(X, Y, Z)$ and I_x, I_y, I_z are the principal moments of inertia of the body. In (1) both $\boldsymbol{M}$ and ω are expressed in the body axes reference frame. The orientation of T_I relative to T_B is obtained through three successive rotations and the resulting coordinate transformation matrix *T* is given by (let $c \triangleq \mathrm{Cos}$, $s \triangleq \mathrm{Sin}$):

$$\mathbf{T} = \begin{vmatrix} c\theta_3\, c\theta_2 & s\theta_3\, c\theta_1 + c\theta_3\, s\theta_2\, s\theta_1 & s\theta_3\, s\theta_1 - c\theta_3\, s\theta_2\, c\theta_1 \\ -s\theta_3\, c\theta_2 & c\theta_3\, c\theta_1 - s\theta_3\, s\theta_2\, s\theta_1 & c\theta_3\, s\theta_1 + s\theta_3\, s\theta_2\, c\theta_1 \\ s\theta_2 & -c\theta_2\, s\theta_1 & c\theta_2\, c\theta_1 \end{vmatrix} \quad \ldots (2)$$

In other terms, if **w** is an arbitrary vector, its components to $[w]$ are transformed from T_b to T_I through the relation:

$$[w]_{T_I} = T[w]_{T_B} \quad \ldots (3)$$

In the following, for simplicity, we will use the notation $[w] \equiv [w]_{T_B}$. It is important to express the angular velocity components $\omega_x, \omega_y, \omega_z$ in terms of the time derivatives of Euler angles $\dot{\theta}_1$, $\dot{\theta}_2$ and $\dot{\theta}_3$. The result is:

$$\begin{cases} \omega_x = \dot{\theta}_1 + \dot{\theta}_3\,\mathrm{Sin}\,\theta_2 \\ \omega_y = \dot{\theta}_2\,\mathrm{Cos}\,\theta_1 - \dot{\theta}_3\,\mathrm{Cos}\,\theta_2\,\mathrm{Sin}\,\theta_1 \\ \omega_z = \dot{\theta}_2\,\mathrm{Sin}\,\theta_1 + \dot{\theta}_3\,\mathrm{Cos}\,\theta_2\,\mathrm{Cos}\,\theta_1 \end{cases} \quad \ldots (4)$$

The inverse relationship is given by:

$$\begin{cases} \dot{\theta}_1 = \omega_x + \omega_y\,\mathrm{Sin}\,\theta_1\,\mathrm{Tan}\,\theta_2 - \omega_z\,\mathrm{Cos}\,\theta_1\,\mathrm{Tan}\,\theta_2 \\ \dot{\theta}_2 = \omega_y\,\mathrm{Cos}\,\theta_1 + \omega_z\,\mathrm{Sin}\,\theta_1 \\ \dot{\theta}_3 = -\omega_y\,\mathrm{Sin}\,\theta_1\,\mathrm{Sec}\,\theta_2 + \omega_z\,\mathrm{Cos}\,\theta_1\,\mathrm{Sec}\,\theta_2 \end{cases} \quad \ldots (5)$$

which can be written in matrix form as:

$$[\dot{\theta}] = \mathbf{E}[\omega] \quad \ldots (6)$$

where

$$\mathbf{E} = \begin{bmatrix} 1 & \mathrm{Sin}\,\theta_1\,\mathrm{Tan}\,\theta_2 & -\mathrm{Cos}\,\theta_1\,\mathrm{Tan}\,\theta_2 \\ 0 & \mathrm{Cos}\,\theta_1 & \mathrm{Sin}\,\theta_1 \\ 0 & -\mathrm{Sin}\,\theta_1\,\mathrm{Sec}\,\theta_2 & \mathrm{Cos}\,\theta_1\,\mathrm{Sec}\,\theta_2 \end{bmatrix} \quad \ldots (7)$$

Correspondingly, Equation (1) may be rearranged in the form:

$$[M] = I[\dot{\omega}] + \Omega I[\omega] \quad \ldots (8)$$

where

$$\mathbf{I} \triangleq \begin{bmatrix} I_x & 0 & 0 \\ 0 & I_y & 0 \\ 0 & 0 & I_z \end{bmatrix} \quad ; \quad \Omega \triangleq \begin{bmatrix} 0 & -\omega_z & \omega_y \\ \omega_z & 0 & -\omega_x \\ -\omega_y & \omega_x & 0 \end{bmatrix} \quad \ldots (9)$$

To get a more compact form define a state vector

$$\mathrm{x} \triangleq \begin{bmatrix} \boldsymbol{\theta} \\ \boldsymbol{\omega} \end{bmatrix} \quad \ldots (10)$$

Then Equations (6) and (8) become

$$\dot{\mathrm{x}} = \boldsymbol{f}(\boldsymbol{x}, \boldsymbol{M}) \quad \ldots (11)$$

In the following we assume that the only external moments are given by the control system, the disturbance torques being negligible. Note that given the control laws $M_x(t)$, $M_y(t)$, $M_z(t)$, Equation (11) amounts to a set of six first order nonlinear differential equations in the six unknowns θ_1, θ_2, θ_3, ω_x, ω_y, ω_z and initial conditions θ_{1_o}, θ_{2_o}, θ_{3_o}, ω_{x_o}, ω_{y_o}, ω_{z_o}.

3.0 PROBLEM STATEMENT

We assume that the spacecraft is constituted by a payload cylindrical module and a service module, which provides the basic spacecraft functions. The service module includes a sun shield with an array of solar cells and various subsystems for thermal control, data handling, power conditioning, etc. The spacecraft must perform a reorientation manoeuvre characterised by a pointing direction of the payload with respect to the T_I reference frame. During the manoeuvre the spacecraft must avoid different pointing constraints and, at the same time, guarantee a minimum angle between the solar cell array and the Sun. For mathematical convenience we introduce a payload unit vector

https://doi.org/10.1017/S0001924000005030 Published online by Cambridge University Press

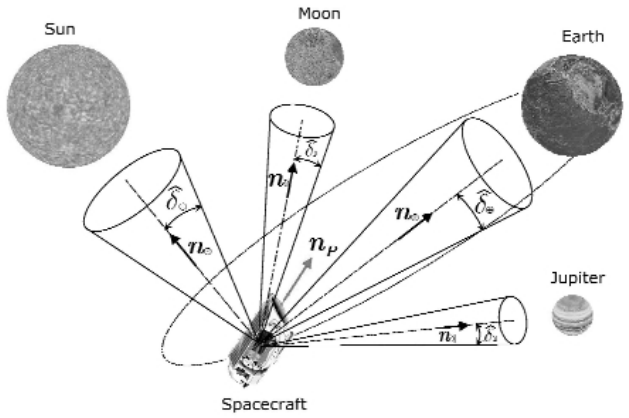


Figure 1. Sketch of the "forbidden cones".

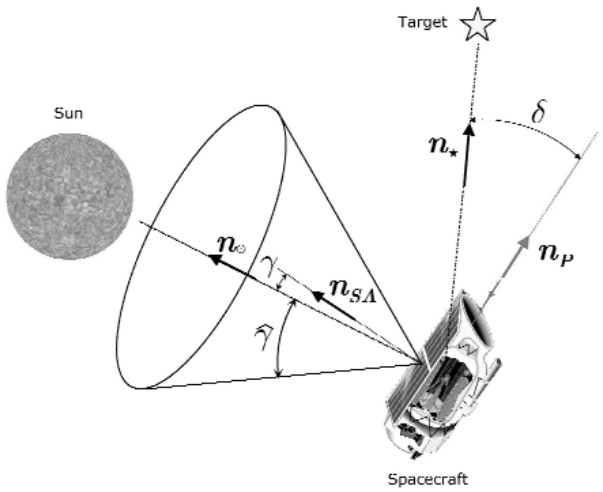


Figure 2. Geometric constraint due to the solar array pointing requirement.

and a solar array unit vector $\mathbf{n}_{SA}$. Both are fixed with respect to the spacecraft. The pointing constraints are specified in terms of m 'forbidden' directions with respect to the inertial frame and serve to avoid that the payload is damaged by bright sky regions (due to the Sun or other celestial bodies). This is equivalent to guarantee that during the whole manoeuvre *i*) $\mathbf{n}_p$ remains outside the m cones generated around the forbidden directions and *ii*) $\mathbf{n}_{SA}$ lies inside a suitable cone generated around the sun direction. Undesired space orientations are expressed through mathematical inequalities of the type

$$\delta_i \triangleq \mathrm{Arccos}(\mathbf{n}_P \cdot \mathbf{n}_i) > \hat{\delta}_i \qquad \text{for } i = 1,\ldots,m \qquad \ldots (12)$$

In particular, Fig. 1 shows the pointing constraints due to Sun, Earth, Moon and Jupiter.

Also, the constraint due to the solar array pointing requirement is expressed by:

$$\gamma \triangleq \mathrm{Arccos}(\mathbf{n}_{SA} \cdot \mathbf{n}_\odot) < \hat{\gamma} \qquad \ldots (13)$$

where angle $\hat{\gamma}$ is shown in Fig. 2.

Assume that the spacecraft has to align its payload with a target direction. (defined through the unit vector $\mathbf{n}_\star$) whose components are known in the T_I reference frame. The control system must assure that the target is caught and maintained within specified limits. This amounts to stating that, at the end of the manoeuvre, both the final angle δ_f between the target and the payload and the angular velocity of the spacecraft ω_f must be sufficiently 'small', i.e.

$$\delta_f \le \delta^{\max} \qquad \ldots (14)$$

$$\|\boldsymbol{\omega}_f\| \le \omega^{\max} \qquad \ldots (15)$$

where

$$\delta \triangleq \mathrm{Arccos}(\mathbf{n}_P \cdot \mathbf{n}_\star) \qquad \ldots (16)$$

The problem consists of finding a suitable control law in the form

$$\begin{cases} M_x = M_x(t) \\ M_y = M_y(t) \\ M_z = M_z(t) \end{cases} \qquad \ldots (17)$$

such that the target is reached within the prescribed requirements (given by Equations (14)-(15)) and the constraints (12) and (13) are met along the spacecraft trajectory.

4.0 THE CONTROL LOGIC

To proceed, we choose an hybrid combination of gas jet and FEEP thrusters that results in a discrete/continuous control law. The motivation is that gas jet based controllers allow rapid reorientation manoeuvres with an angular resolution that is insufficient for many practical situations. On the other hand, FEEP thrusters can give a continuous, small torque that is very well suited for fine spacecraft positioning. The two control logics may be integrated through a potential function $V(\mathbf{x})$ as follows:

$$V(\mathbf{x}) = \begin{cases} V_\delta & \text{if } \delta > \varepsilon \\ V_\delta + V_\omega & \text{if } \delta \le \varepsilon \end{cases} \qquad \ldots (18)$$

where

$$V_\delta = \frac{\delta^2}{2}\left[1 + \frac{1}{(\hat{\gamma}-\gamma)^2} + \sum_{i=1}^{m} \frac{1}{(\delta_i - \hat{\delta}_i)^2}\right] \qquad \ldots (19)$$

$$V_\omega = \frac{1}{2\eta M^{\max}} [\omega]^T I [\omega] \qquad \ldots (20)$$

and ε is a switching angle establishing the transition between discrete and continuous control. In essence Equation (18) says that the gas jet-based controllers serve to quickly drive the payload towards the target direction (in fact the minimum of the potential function occurs for $\delta = 0$). On the other hand the continuous control is used in the proximity of the desired pointing direction to give the latter an adequate accuracy (note that the potential function contains a term involving the angular velocity and, in particular, it achieves a minimum for $\delta = 0$ and $\|\boldsymbol{\omega}\| = 0$). The terms with γ and δ_i in Equation (19) guarantee that the constraints (12) and (13) are satisfied. Also, in Equation (20) M^{max} is the maximum torque produced by FEEP thrusters and is introduced to non-dimensionalise V_ω. Finally, η is an non-dimensional parameter that plays an important role in the definition of the continuous control law, as discussed soon. It should be noted that both V_δ and V_ω are function of the state vector $\mathbf{x}$ [indeed $\delta = \delta(\theta)$ via Equations (16) and (3)]. In particular, the potential function has the following characteristics:

$$V(\mathbf{x})\big|_{\mathbf{x}=\mathbf{x}_f} = 0 \qquad \ldots (21)$$

$$V(\mathbf{x}) > 0 \quad , \quad \forall\, \mathbf{x} \neq \mathbf{x}_f \qquad \ldots (22)$$

$$V(\mathbf{x}) \to \infty \quad \text{as } \|\mathbf{x}\| \to \infty \qquad \ldots (23)$$

https://doi.org/10.1017/S0001924000005030 Published online by Cambridge University Press

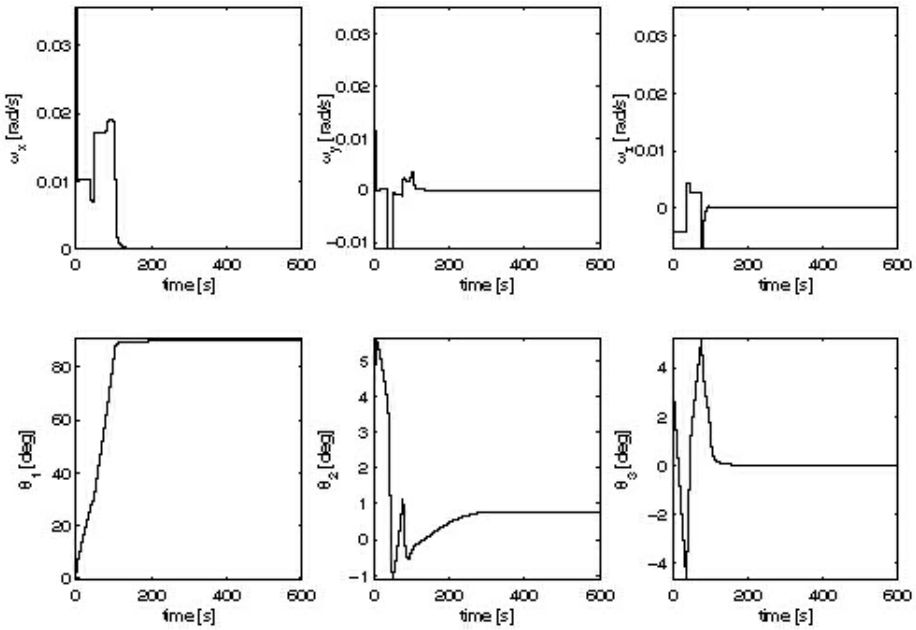


Figure 3. Time histories of angular velocities and attitude angles.

By virtue of Lyapunov's direct method, the further condition

$$\dot{V}(\mathbf{x}) < 0 \quad , \quad \forall\ \mathbf{x} \neq \mathbf{x}_f \qquad \ldots (24)$$

is sufficient to guarantee that the equilibrium point $\boldsymbol{x}_f$ is globally asymptotically stable. For this reason, the control time history Equation (17) must assure that the inequality in Equation (24) is met.

4.1 Discrete control

As long as δ is greater than the switching angle ε, gas jet thrusters are employed for control purposes. The thrusters give constant and independent torques along the three body axes of the spacecraft and are activated with an on-off logic. In this phase the spacecraft dynamics is made of either open loop ($\boldsymbol{M} = 0$) or controlled trajectory arcs ($\boldsymbol{M} \neq 0$) according to whether condition (24) is met or not. More precisely, for $\dot{V}_\delta > 0$ the jet thrusters are activated until Equation (24) is reestablished. Note that:

$$\dot{V}_\delta = \nabla V_\delta [\dot{\theta}] = \nabla V_\delta \mathbf{E}[\omega] \qquad \ldots (25)$$

where:

$$\nabla V_\delta = \delta\left[1 + \frac{1}{(\hat{\gamma} - \gamma)^2} + \sum_{i=1}^{m} \frac{1}{(\delta_i - \hat{\delta}_i)^2}\right]\nabla\delta + \frac{\delta^2}{(\hat{\gamma} - \gamma)^3}\nabla\gamma - \sum_{i=1}^{m} \frac{\delta^2}{(\delta_i - \hat{\delta}_i)^3}\nabla\delta_i \qquad \ldots (26)$$

If condition Equation (24) is violated, the time derivative of Euler's angles are forced to follow a desired trajectory, namely:

$$[\dot{\theta}^d] = -\varpi_p \mathrm{T\,anh}[(\delta/\delta_p)^2]\frac{(\nabla V_\delta)^T}{\|\nabla V_\delta\|} \qquad \ldots (27)$$

where $\varpi = \varpi_p$ Tanh $[(\delta/\delta_p)^2]$ is a shaping function whose purpose is

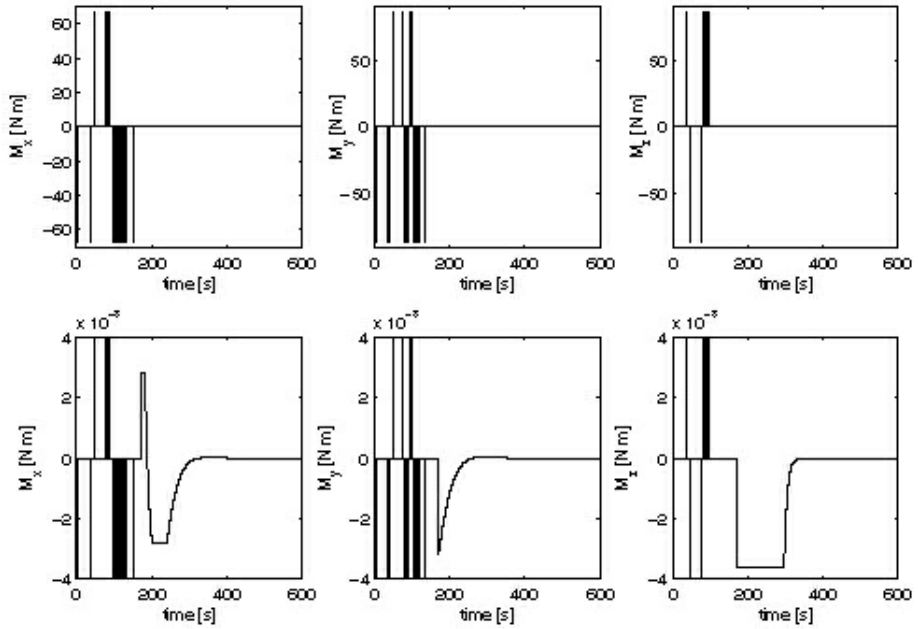


Figure 4. Time histories of control torques. The different scale in the lower graphs emphasises the contribution of the FEEP thrusters.

https://doi.org/10.1017/S0001924000005030 Published online by Cambridge University Press

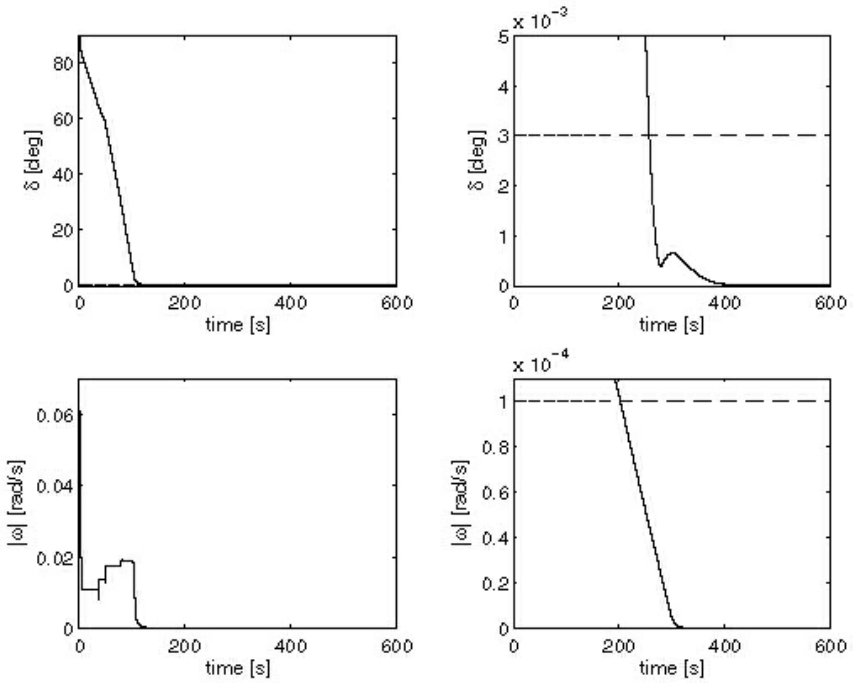


Figure 5. Time histories of slew angle and spacecraft angular velocity with the corresponding pointing constraints (dotted line).

to drive the system response towards the final equilibrium position by suitable choice of the design parameters ϖ_p and δ_p. The rationale in its choice is this: the term $\varpi = \varpi_p$ Tanh $[(\delta/\delta_p)^2]$ smoothly slows down the body rates as the spacecraft approaches the final equilibrium point. This happens through the terms ϖ_p and δ_p that ultimately affect the velocity (through the parameter ϖ_p) and the angular deceleration (through the parameter δ_p). These parameters must be selected using a trial and error procedure. Note also that the term $(\nabla V_\delta)^T \|\nabla V_\delta\|$ is the unit vector of the potential function gradient. Accordingly, the minus sign in Equation (27) renders $\dot{V}_\delta < 0$ thus guaranteeing condition Equation (24).

The corresponding desired angular velocity components are found from Equation (6)

$$[\omega^d] = -\varpi \, \boldsymbol{E}^{-1} \frac{(\nabla V_\delta)^T}{\|\nabla V_\delta\|} \quad \ldots (28)$$

The spacecraft's actual angular velocity follows the desired one provided that

$$I[\dot{\omega}] + \Omega I[\omega] - [M] = I[\dot{\omega}^d] \quad \ldots (29)$$

However Equation (29) cannot be exactly satisfied by a discontinuous controller. The corresponding linear approximation is

$$I\left\{[\dot{\omega}] - [\dot{\omega}^d]\right\} = [M] \quad \ldots (30)$$

from which an estimate of the thruster pulse width is obtained via the simplified relations:[6] ... (31)

$$\Delta t_x = |\omega_x^d - \omega_x| \frac{I_x}{M_x} \quad ; \quad \Delta t_y = |\omega_y^d - \omega_y| \frac{I_y}{M_y} \quad ; \quad \Delta t_z = |\omega_z^d - \omega_z| \frac{I_z}{M_z}$$

and a thruster is activated only if the generic Δt_i is greater than the minimum pulse width.

4.2 Continuous control

It has been stated previously that a precise pointing direction cannot be achieved through a discrete control. For this reason, the final part of the manoeuvre is implemented with FEEP thrusters. In particular, when $\delta \leq \varepsilon$ the continuous control logic is engaged. Note that from Equations (18)-(20) one has

$$\dot{V} = \frac{1}{\eta M^{\max}} [\dot{\omega}]^T \boldsymbol{I}[\omega] + \nabla V_\delta \boldsymbol{E}[\omega] \quad \ldots (32)$$

To satisfy Equation (24) it is sufficient to impose that

$$\dot{V} = -k[\omega]^T [\omega] \quad \ldots (33)$$

where $k > 0$ is a design parameter. Bearing in mind Equation (8), the following control law is easily derived from (32) and (33):

$$[M] = -\eta M^{\max} k[\omega] - \eta M^{\max} \boldsymbol{E}^T (\nabla V_\delta)^T + \Omega \boldsymbol{I}[\omega] \quad \ldots (34)$$

where ∇V_δ is given by Equation (26). It should be noted that the independent parameters η and k allow one to tune the relative importance of the three terms in Equation (34). Both parameters are chosen with a trial and error approach. Note however that, loosely speaking, 'high' values of the parameter k correspond to a slow spacecraft movement, whereas 'small' values of k correspond to a rapid, fine pointing maneuver. Finally, when the required control torques are out of the thruster operative range, Equation (34) is modified as follows

$$\begin{cases} M_i = 0 & \text{if } |M_i| < M^{\min} \\ M_i = \text{sgn}(M_i) M^{\max} & \text{if } |M_i| > M^{\max} \end{cases} \quad \ldots (35)$$

where M_i is the control torque relative to the generic axis, M^{min} is the minimum torque provided by FEEP thrusters and sig(.) is the signum function.

5.0 CASE STUDY

To illustrate the above methodology we discuss a large angle reorientation manoeuvre for a space telescope. In particular, we consider the geometric-inertial data of the Infrared Space Observatory (ISO)[10] summarised in Table 1.

assumed that the payload unit vector $\mathbf{n_p}$ and the solar array unit vector $\mathbf{n_{SA}}$ coincide with the third and first unit vectors of $T_B(x,y,z)$, *i.e.*

$$\mathbf{n_p} \equiv \mathrm{k} \quad \ldots (36)$$

https://doi.org/10.1017/S0001924000005030 Published online by Cambridge University Press

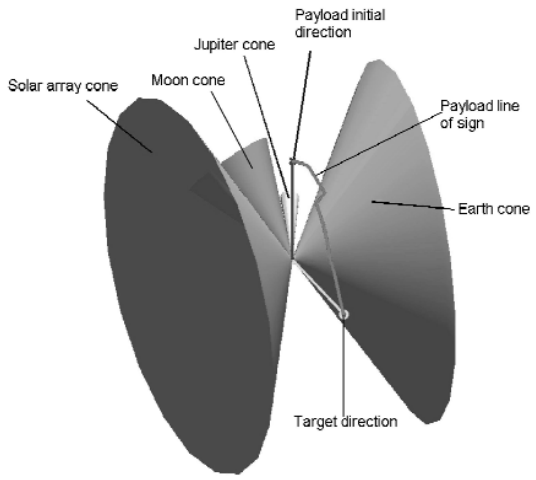


Figure 6. Spacecraft reorientation manoeuvre with avoidance of prescribed obstacles.

$$\mathbf{n_{SA}} \equiv \mathbf{i} \qquad \ldots (37)$$

Using Equations (2)-(3) the components of $\mathbf{n_P}$ and $\mathbf{n_{SA}}$ are easily expressed in the inertial frame

$$[n_P]_{T_I} = \boldsymbol{T}\begin{bmatrix}0\\0\\1\end{bmatrix} = \begin{bmatrix}-\mathrm{Sin}\,\theta_2\,\mathrm{Cos}\,\theta_1\,\mathrm{Cos}\,\theta_3 + \mathrm{Sin}\,\theta_1\,\mathrm{Sin}\,\theta_3\\ \mathrm{Sin}\,\theta_2\,\mathrm{Cos}\,\theta_1\,\mathrm{Sin}\,\theta_3 + \mathrm{Sin}\,\theta_1\,\mathrm{Cos}\,\theta_3\\ \mathrm{Cos}\,\theta_1\,\mathrm{Cos}\,\theta_2\end{bmatrix} \qquad \ldots (38)$$

$$[n_{SA}]_{T_I} = \boldsymbol{T}\begin{bmatrix}1\\0\\0\end{bmatrix} = \begin{bmatrix}\mathrm{Cos}\,\theta_2\,\mathrm{Cos}\,\theta_3\\ -\mathrm{Cos}\,\theta_2\,\mathrm{Sin}\,\theta_3\\ \mathrm{Sin}\,\theta_2\end{bmatrix} \qquad \ldots (39)$$

To be specific, we assume that the pointing constraints are due to Sun, Earth, Moon and Jupiter ($m = 4$). Accordingly, bearing in mind Equation (12) and referring to Fig. 1, one has:

$$\begin{cases}\delta_\odot \triangleq \arccos(\mathbf{n_P}\cdot\mathbf{n_\odot}) > \hat{\delta}_\odot\\ \delta_\leftmoon \triangleq \arccos(\mathbf{n_P}\cdot\mathbf{n_\leftmoon}) > \hat{\delta}_\leftmoon\\ \delta_\oplus \triangleq \arccos(\mathbf{n_P}\cdot\mathbf{n_\oplus}) > \hat{\delta}_\oplus\\ \delta_\jupiter \triangleq \arccos(\mathbf{n_P}\cdot\mathbf{n_\jupiter}) > \hat{\delta}_\jupiter\end{cases} \qquad \ldots (40)$$

The angular constraints for the reference spacecraft are summarised in Table 2 above. The target has the following pointing constraints. and the thruster characteristics are shown in Table 3 below.

$$\ddot{a}^{\max} = 0.003\,\mathrm{deg} \cong 5\times10^{-5}\,\mathrm{rad}$$

$$\dot{u}^{\max} = 1\times10^{-4}\,\mathrm{rad/s}$$

Table 1
Spacecraft geometric-inertial data

Parameter	Value
height	5·3m
width	3·6m
depth	2·8m
launch mass	2,400kg
I_x	6,587kgm^2
I_y	7,526kgm^2
I_z	3,813kgm^2

Table 2
Angular constraints (from Leech *et al*[10])

Angle	Value (deg)
$\hat{\delta}_\odot$	15
$\hat{\delta}_\leftmoon$	24
$\hat{\delta}_\oplus$	58
$\hat{\delta}_\jupiter$	7
$\hat{\gamma}$	30

The initial conditions are: $\omega_{x_o} = \omega_{y_o} = \omega_{x_o} = 0{\cdot}0035$rad/s, $\theta_{1_o} = \theta_{2_o} = \theta_{3_o} = 0$ It is assumed that the spacecraft must align its payload with the target direction $[n_\star]_{T_I} = [010]^T$, which amounts to a 90° total slew manoeuvre. The design parameters are as follows: $\delta_p = 0{\cdot}06$, $\varpi_p = 0{\cdot}019$rad/s, $k = 500$s and $\eta = 300$. Finally, the switching angle is fixed to $\varepsilon = 0{\cdot}1°$, in keeping with the typical tolerance achievable with reaction jets. Figures 3 and 4 show the time histories of angular velocities, attitude angles and control torques.

In particular, the lower graphs in Fig. 4 emphasises the role of the FEEP thrusters in the terminal phase of the manoeuvre.

Figure 5 shows the slew angle and the modulus of the spacecraft angular velocity and the corresponding pointing constraints. It should be noted that, at the end of the manoeuvre, both constraints are met: in particular the slew angle becomes smaller than the required tolerance in near 250s .

The whole reorientation manoeuvre is depicted in Fig. 6, where the pointing constraints are shown and the effectiveness of the algorithm is demonstrated.

6.0 CONCLUSIONS

A new method has been proposed that allows large angle slew manoeuvres with pointing constraints. The problem of attitude control is formulated and solved through potential functions that considerably simplify spacecraft reorientation manoeuvres with autonomous re-targeting capabilities. Spacecraft reorientation is achieved in two integrated steps by means of a discrete/continuous control law. The initial rapid slew manoeuvres are obtained through reaction jets with a discrete control law and an error tolerance of near 0·1°. In the ter-

Table 3
Thruster characteristics

Gas jet trusters	
thrust level	24N
minimum pulse width	0·01s
specific impulse	230s
$\overline{M_x}$	67·2N·m
$\overline{M_y}$	86·4N·m
$\overline{M_z}$	86·4N·m
FEEP trusters	
Specific impulse	6,000s
$M_x^{\min}$	2·8×10^{-6}N·m
$M_x^{\max}$	2·8×10^{-3}N·m
$M_y^{\min}$	3·6×10^{-6}N·m
$M_y^{\max}$	3·6×10^{-3}N·m
$M_z^{\min}$	3·6×10^{-6}N·m
$M_z^{\max}$	3·6×10^{-3}N·m

https://doi.org/10.1017/S0001924000005030 Published online by Cambridge University Press

minal phase FEEP thrusters are activated and a continuous control law is employed. Accurate pointing capabilities are possible with thrust modulation in the 1μN-1mN range. The whole slew manoeuvre is completed in a few hundred seconds and the pointing tolerance is well below 0·003°, typical of a space telescope. The control torques are evaluated in closed form, thus facilitating the on-board implementation with reduced software requirements. Autonomous avoidance of undesired space orientations is easily formulated and constraints due to the solar array pointing requirements are satisfied. Note that a problem may arise in case a failure in the attitude control system causes the spacecraft attitude to move into one of the forbidden cones, or, more likely, the solar panel pointing vector to move outside the sun pointing cone created by the potential function. In that case, before the redundant hardware is employed, it is necessary to verify that the payload and the solar array unit vectors meet all the constraints, otherwise the control system would force the spacecraft attitude to stay within the forbidden cone or keep the solar panel facing away from the sun.

A detailed case study has been presented to validate the proposed approach.

REFERENCES

1. SORENSON, A. M. ISO Attitude maneuver strategies, American Astronautical Society, Paper AAS 93-317, 1993, pp 975-987.
2. FRAKES, J.P., HENRETTY, D.A., FLATLEY, T.W., MARKLEY, F.L., SAN, J.K. and LIGHTSEY, E.G. SAMPEX Science pointing with velocity avoidance, AAS/AIAA Spaceflight Mechanics Meeting, Paper AAS 92-182, 1992, pp 949-966.
3. SINGH, G., MACALA, G., WONG, E. and RASMUSSEN, R. A Constraint monitor algorithm for the Cassini spacecraft, AIAA Guidance, Navigation & Control Conference, 1997, Reston, VA, pp 272-282.
4. HABLANI, H. B. Attitude commands avoiding bright objects and maintaining communication with ground station, *J Guidance, Control, and Dynamics*, November-December 1999, **22**, (6), pp 759-767.
5. MCINNES, C.R. Large angle slew manoeuvres with autonomous sun vector avoidance, *J Guidance, Control and Dynamics*, 1994, **17**, (4), pp 875-877.
6. RADICE, G. and MCINNES, C.R. Contrained on-board attitude control using gas jet thrusters, *Aeronaut J*, December 1999, **103**, (1030), pp 549-556.
7. WIE, B. and BARBA, P.M. Quaternion feedback for spacecraft large angle maneuvers, *J Guidance, Control, and Dynamics*, May-June 1985, **8**, (3), pp 360-365.
8. MARCUCCIO, S., GENOVESE, A. and ANDRENUCCI, M. Experimental performance of field emission microthrusters, *J Propulsion and Power*, September-October 1998, **14**, (5), pp 774-781.
9. MARCUCCIO, S., GENOVESE, A. and ANDRENUCCI, M. FEEP Microthruster technology status and prospects, Proceedings of the 48th International Astronautical Federation Congress, 1997, Turin, Italy.
10. LEECH, K. and POLLOCK, A.M.T. ISO – The Satellite and its data, **II** SAI/99-082/Dc, July 2000, Space Science Department of ESA, Villafranca, P.O. Box 50727, E-28080 Madrid, Spain, Version 1.0.

https://doi.org/10.1017/S0001924000005030 Published online by Cambridge University Press